Identification of inner and outer shells of double-wall carbon nanotubes using high-pressure Raman spectroscopy

D. Christofilos,[1,*] J. Arvanitidis,[1,2] G. A. Kourouklis,[1] S. Ves,[3] T. Takenobu,[4] Y. Iwasa,[4] and H. Kataura[5]
[1]*Physics Division, School of Technology, Aristotle University of Thessaloniki, 54124 Thessaloniki, Greece*
[2]*Department of Applied Sciences, Technological Educational Institute of Thessaloniki, 57400 Sindos, Greece*
[3]*Physics Department, Aristotle University of Thessaloniki, 54124 Thessaloniki, Greece*
[4]*Institute for Materials Research, Tohoku University, 2-1-1 Katahira, Aoba-ku, Sendai 980-8577, Japan and CREST, Japan Science and Technology Corporation, Kawaguchi 332-0012, Japan*
[5]*National Institute of Advanced Industrial Science and Technology (AIST), 1-1-1 Higashi, Tsukuba, Ibaraki 305-8562, Japan*
(Received 13 April 2007; revised manuscript received 12 July 2007; published 7 September 2007)

The high-pressure Raman response of double-wall carbon nanotubes (DWCNTs) in the radial breathing mode (RBM) frequency region can be used for the identification of both the inner and their respective outer tubes. A simple anharmonic model of this system demonstrates that the pressure response of the inner tube in a DWCNT is uniquely defined by the inner-outer tube spacing. Consequently, a plot of the normalized pressure coefficients of the inner tube RBM frequencies as a function of their ambient pressure frequency serves as a map which allows the identification of unknown DWCNTs. The present experimental results form the basis of such a plot.

DOI: 10.1103/PhysRevB.76.113402 PACS number(s): 78.67.Ch, 62.50.+p, 63.22.+m, 78.30.Na

The intense interest of pure sciences and technology has been recently focused in the nanoscopic regime of matter, where the physical and chemical properties deviate significantly from those commonly encountered in the bulk state. The development of this scientific area is facilitated by the combination of constantly improving preparation procedures and experimental techniques allowing the direct or indirect visualization of nano-objects. In the field of carbon nanotubes, their size-dependent peculiar electronic structure originating from the quasi-one-dimensional electron confinement[1,2] has established the use of optical techniques for their selective probing.[3,4] In particular, Raman spectroscopy has been proven to be a valuable tool in carbon nanotube research owing to the inversely proportional relation between the radial breathing mode (RBM) frequency and the tube diameter, which discriminates tubes of different sizes being resonantly excited.[5] The accumulated theoretical and experimental findings for single-wall carbon nanotubes (SWCNTs) have led to the development and steady improvement of several maps that allow the indexing of the tubes comprising a SWCNT material.[3,6–9] In the case of double-wall carbon nanotubes (DWCNTs), the determination of their constituting inner and outer tubes is strongly hindered by the existence of the inner-outer tube (intratube) interaction. This leads to the modification of the resonance conditions and the intratube interaction-dependent upshift of the RBM frequencies.[10–12] Consequently, several peaks from those appearing in the RBM region do not really originate from different inner tubes but rather from the same inner tube being encapsulated in outer tubes of different diameters (split RBM components).[13,14] The initially suggested maximum splitting of $\sim 5\ \mathrm{cm}^{-1}$ for the inner tube RBM frequencies[10] is extended up to $30\ \mathrm{cm}^{-1}$, at least for the case of the (6,4) and (6,5) inner nanotubes.[13]

In this Brief Report, the experimental pressure response of the inner tube RBMs in DWCNTs, as expressed by their normalized pressure coefficients (Γ_i) obtained at different resonance conditions, is compared with the results from a simple anharmonic model. We demonstrate that the Γ_i vs ω plot provides a tool for the determination of the inner tubes present in DWCNT samples. Furthermore, it allows the estimation of the DWCNT intratube spacings for each inner tube and, consequently, its associated outer tubes, which could not be confidently accomplished before solely by means of Raman spectroscopy.

The studied DWCNT material has been synthesized by means of the C_{60}-peapod conversion process, following the procedure of Bandow *et al.*[15] Details of the sample preparation and the extensive characterization of the starting SWCNT material, the intermediate step peapods, and the resulting DWCNTs by means of transmission electron microscopy, x-ray diffraction, and Raman spectroscopy can be found elsewhere.[1,14,16–20] The Raman spectra in the RBM frequency region of the inner tubes for various excitation lines are illustrated in Fig. 1. They consist of numerous well-resolved narrow peaks, which exhibit significant intensity redistribution on going from 1.83 to 2.41 eV excitation due to the different resonance conditions. Their large number is attributed to the split RBM components mentioned above.[13,14]

In Fig. 2, we compile the experimentally obtained normalized pressure slopes, $\Gamma_i=(1/\omega_i)(\partial\omega_i/\partial P)$, of the inner tube RBMs as a function of their frequency ω_i. The Γ_i values obtained for four different excitation energies (2.41, 1.83, 1.96, and 1.92 eV) exhibit an overall decrease with increasing ω, which is attributed to the higher stiffness of the smaller diameter tubes. Noticeably, the data are distributed in five groups (labeled by the letters a–e), in which Γ_i increases with ω_i. Each group has been qualitatively attributed to the same inner tube included into outer tubes of different diameters, as well as to appropriate inner-outer tube combinations which fulfill the Γ_i-ω_i increasing trend.[14]

For a better understanding of the underlying mechanisms responsible for the observed behavior, we have developed a simple phenomenological model where the elastic properties

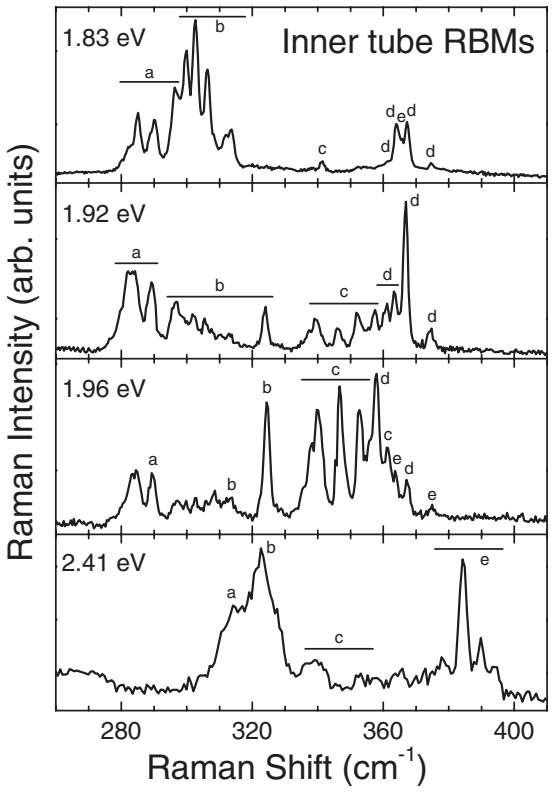

FIG. 1. Raman spectra of DWCNTs in the RBM frequency region of the inner tubes for various excitation lines at ambient conditions. RBM peaks belonging to each of the five data distributions presented in Fig. 2 are labeled by the letters a–e, accordingly.

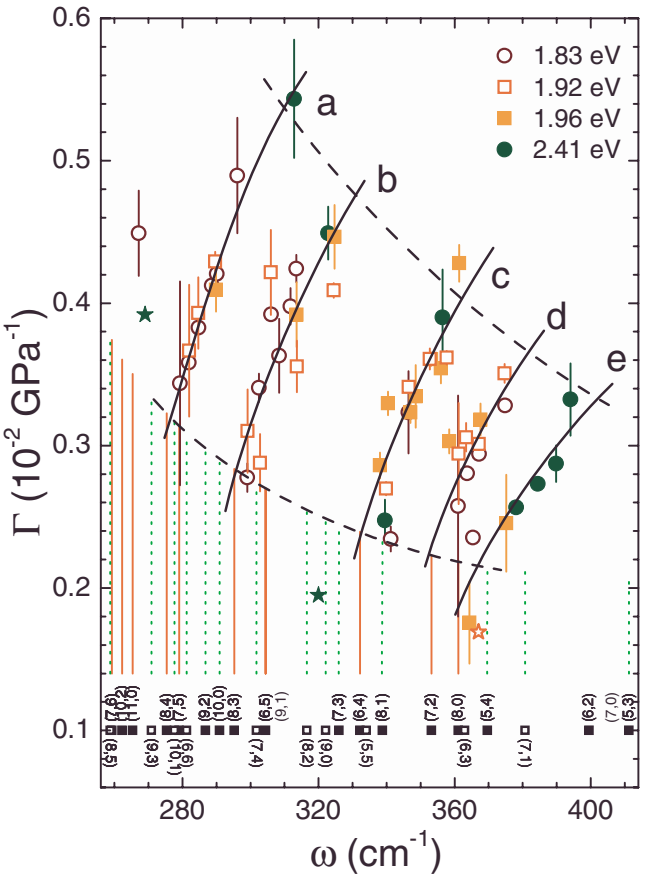

FIG. 2. (Color online) Normalized pressure slopes, $\Gamma_i = (1/\omega_i)(\partial\omega_i/\partial P)$, of the inner tube RBMs in DWCNTs as a function of their frequency for various excitation lines (different symbols). The solid lines through the data emphasize their grouping in five distributions, labeled by the letters a–e. The star symbols correspond to data obtained from Ref. 24 with excitation at 514.5 (solid stars) and 647.1 nm (open star). All the carbon nanotubes with diameters of 0.55–0.90 nm along with their chiral indices (n,m) are appropriately included in the lower part of the figure by means of the frequency-diameter relations given by Fantini *et al.* (Ref. 7). The vertical lines mark the tubes which are in resonance with the red (solid lines) or the green excitation (dotted lines).

of a nanotube are approximated by those of its cross section, modeled as a ring of carbon atoms in a regular polygonal arrangement. We assume only first neighbor interactions described by a Lennard-Jones (LJ) potential, where the equilibrium length of the C–C bond is assumed to be 0.142 nm. The fully symmetric radial [hereafter radial breathinglike mode (RBLM)] and the in-plane tangential [hereafter G^--like mode (GLM)] vibrations of the atoms in the ring correspond to the RBM and the G^- mode of a carbon nanotube, respectively (Fig. 3, inset). The restoring force for the RBLM (GLM) decreases (increases) with increasing tube diameter D. For $D \rightarrow \infty$, the RBLM frequency tends to zero, while, at the same time, we require that the GLM frequency attains the value of the tangential mode of graphite ($\sim$1580 cm^{-1}). This requirement allows the determination of the energy LJ parameter in the model. We also assume that the applied pressure is exerted radially on an effective area of 0.142×0.142 nm^2 for each atom and it does not induce any shape distortion of the ring. Upon pressure application, the ring diameter of the relaxed system is calculated, allowing the determination of the RBLM force constant at the new equilibrium position and hence the ω_{RBLM} value. The calculation of the RBLM frequency and its pressure response is considerably simplified taking into account the radial symmetry of the system. This allows the description of the ring by an equivalent anharmonic oscillator (of LJ type) of length equal to the ring radius and the same energy LJ parameter with that determined for the ring.

A combination of two such anharmonic oscillators, interacting through another LJ potential with an equilibrium distance of 0.344 nm (the turbostratic constraint of graphite at ambient conditions), has been used to calculate the pressure dependence of the RBLM frequencies of the inner and outer tubes constituting a DWCNT. The combination of the two RBLMs results in a low frequency mode, where the two oscillators are in phase, and a higher frequency mode where they are out of phase. The model can be easily generalized to describe a carbon nanotube system of an arbitrary number of walls (multiwall carbon nanotube). The energy parameter of the LJ potential describing the coupling of the anharmonic oscillators at the equilibrium distances (0.344 nm) is determined by assuming that for a large number of oscillators with infinitely large length, the highest frequency mode should attain the frequency of the B_{2g} mode of graphite (127 cm^{-1}).[21] Despite its apparent simplicity, our model re-

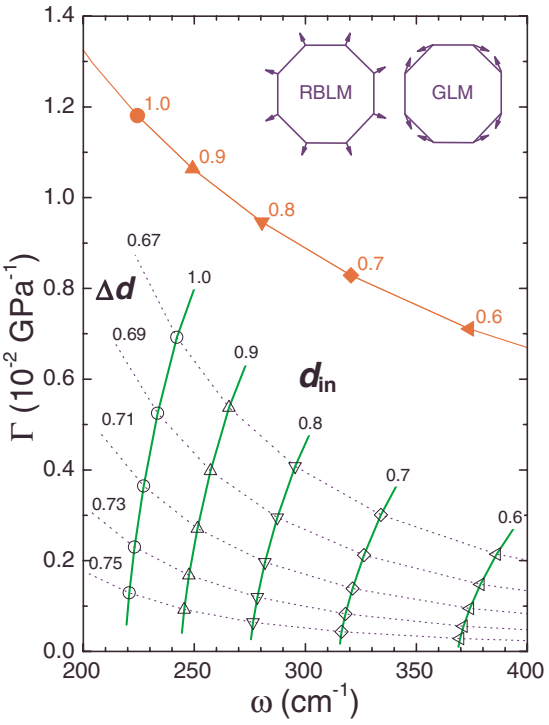

FIG. 3. (Color online) Normalized pressure slopes, $\Gamma_i = (1/\omega_i)(\partial\omega_i/\partial P)$, of the RBLMs of the single ring (solid symbols) and the inner rings comprising the double-ring model system (open symbols). The thick solid lines group data originating from the same inner ring of diameter d_{in} combined with outer rings of different diameters d_{out}, while the dotted lines delineate Γ_i values for inner-outer pairs of constant $\Delta d = d_{\text{out}} - d_{\text{in}}$. All lengths are expressed in nanometers. Inset: RBLM and GLM of a single ring.

produces qualitatively all the size and intratube dispersive characteristics of the RBMs in carbon nanotubes presented in previous theoretical works.[12,22]

In the framework of this model, it is feasible to construct the Γ_i-ω_i plot for inner and outer ring combinations of different diameters d_{in} and d_{out}, respectively. In Fig. 3, the calculated values are plotted for the inner rings with $d_{\text{in}} = 0.6-1.0$ nm and for various inner-outer ring diameter differences (Δd) in the range 0.67–0.75 nm, compatible with the intratube spacing of 0.34–0.38 nm of our sample. The Γ_i values for the inner rings are systematically smaller than those for single rings with the same diameters. This reflects the pressure screening in the interior of the outer tube, in excellent agreement with our experimental findings reported earlier.[23] For a specific inner ring, the decrease of Δd causes the increase of the ring-ring interaction, resulting in the upshift of the RBLM frequency and the more efficient pressure transmission to the inner ring (larger Γ_i). For large Δd values, the frequency becomes equal or even slightly smaller than that of an individual ring of the same diameter as the inner-outer ring interaction causes the contraction of the outer ring and the expansion of the inner one. In this case, the "negative" pressure exerted on the inner ring results in Γ_i values approaching zero or even attaining small negative values. The resulting families are unique for each inner ring enclosed in different outer ones, and families originating from different rings never cross. This holds also for larger Δd values than those depicted in Fig. 3, at least as long as Γ_i is positive.

The theoretically predicted one-to-one correspondence between (ω_i, Γ_i) and $(d_{\text{in}}, \Delta d)$ pairs supports the use of our experimental Γ_i-ω_i plot (Fig. 2) for the identification of both the inner and the outer tube constituting a DWCNT. Comparison of Figs. 2 and 3 reveals a striking similarity between the experimental and the theoretical Γ_i-ω_i plots. Despite the apparent simplicity of the model employed, leading to deviation between the calculated and experimental Γ_i values, their order of magnitude is the same. Therefore, each of the five groups, a–e, originates from one inner tube (or more of very similar diameter) encapsulated in outer tubes of different sizes.

In order to associate the data points in Fig. 2 to specific inner and outer tube combinations, we keep in mind the following considerations. First, the relatively large number of carbon nanotubes with diameters of 0.55–0.90 nm (chiral indices in the lower part of the figure) is significantly reduced by taking into account the resonance conditions, fulfilled within ±0.2 eV, for a given excitation energy (vertical lines in the figure).[3,6,7] Second, the dashed lines, which envelop the main volume of our data, should correspond to the intratube spacing limits (0.34 and 0.38 nm). Third, our model calculations indicate that for intratube spacing close to 0.38 nm (lower dashed line), the inner tube RBM frequency should be close to that of an individual SWCNT of the same diameter, allowing for the identification of the inner tube. Consequently, the data of group a obtained with the red excitation (1.83, 1.92, and 1.96 eV) should originate from the (7,5) and (8,4) inner tubes which have similar diameters. The former is more probable as its resonance matches these excitation energies better. The frequencies of the split components span a range of ~20 cm^{-1}, which corresponds to the encapsulation of this tube in outer tubes with diameters of 1.60–1.52 nm as we move within this group from the lower to the upper dashed line. As for the data point obtained with the green excitation (2.41 eV), it can be tentatively attributed to a split component of the (10,1) inner tube which is upshifted by ~30 cm^{-1}. Nevertheless, the closely lying in diameter (6,6) tube should not be excluded. The (8,3) tube generates the data of group b, at least within the first 10 cm^{-1}, while for larger frequency upshifts, the (6,5) (for higher excitation energies) and (9,1) tubes (for lower excitation energies) also contribute to this group, in accordance with the larger scattering of the data points in this distribution. The data of group c obtained with the red excitation undoubtedly originate from the (6,4) tube. The frequencies of the split components span a range of ~25 cm^{-1}, corresponding to the inner tube encapsulation in outer tubes having diameters of 1.45–1.37 nm. Concerning the data points obtained with the green excitation, the one with the smaller Γ_i is most likely associated with the (8,1) tube while that with larger Γ_i is possibly related to the (7,3) tube. Group d can be assigned to the (7,2) tube, whereas the lower part of group e can be assigned to the (8,0) tube. Finally, the data of group e obtained with green excitation should be attributed to the (5,4) tube enclosed in outer tubes with diameters down to 1.30 nm.

The assignment of the inner tubes and the RBM split components in the studied material is in excellent agreement with the contour plot of the excitation energy vs RBM frequency constructed by Pfeiffer *et al.*[13] for similar DWCNTs. However, in our method, the knowledge of the pressure response for the inner tube RBMs confidently determines the upper and the lower frequency boundaries of the split components in the Raman spectrum of DWCNTs (Fig. 1). This is of great importance whenever split components of different inner tubes overlap in frequency, allowing their precise assignment (groups c–e). In addition, data points lying outside the area determined by the dashed lines in Fig. 2 and groups a and e can also be assigned to a specific pair of tubes. For instance, the lowest point in group e is attributed to the (8,0) tube with an intratube distance of ~0.39 nm, while the point having the lowest frequency is attributed to the (7,6) tube with an intratube distance of ~0.37 nm (d_{out}=1.63 nm). In this context, we can also assign the experimental Γ_i values obtained by Venkateswaran for another DWCNT material (stars in Fig. 2).[24] The first RBM located at 269 cm^{-1} is most probably associated with the (8,5)@(17,6) or the (8,5)@(19,3) DWCNT, the second at 320 cm^{-1} to (7,3)@(15,6) or the (7,3)@(17,3) DWCNT, while the third at 367 cm^{-1} to the (8,0)@(14,6) DWCNT.

Summarizing, a simple and reliable method has been developed that allows the determination of the inner-outer tube combinations comprising a DWCNT material on the basis of a Γ_i-ω_i plot. As the pressure response of the inner tube RBMs bares information for both the inner and the outer tube, the latter could be out of resonance and thus invisible by the wavelength used for the excitation of the Raman spectrum. It must be noted that, although it is not straightforward to attain the pressure response of a sample, even an ambient pressure Raman measurement can be exploited (taking advantage of the presented Γ_i-ω_i plot) to determine the possible inner-outer pairs that correspond to a specific RBM peak. We anticipate that the incorporation in Fig. 2 of additional experimental results originating from different well-characterized DWCNTs and the extension of the excitation wavelength coverage will render the presented Γ_i-ω_i plot a powerful tool for the accurate characterization of carbon nanotube materials.

This work was partly supported by NEDO and MEXT, Japan. The financial support from the Hellenic Ministry of National Education and Religious Affairs and the European Union through the "Pythagoras II" program is greatly acknowledged.

*Author to whom correspondence should be addressed; christof@vergina.eng.auth.gr

[1] H. Kataura, Y. Kumazawa, Y. Maniwa, I. Umezu, S. Suzuki, Y. Ohtsuka, and Y. Achiba, Synth. Met. **103**, 2555 (1999).
[2] F. Wang, G. Dukovic, L. E. Brus, and T. F. Heinz, Science **308**, 838 (2005).
[3] S. M. Bachilo, M. S. Strano, C. Kittrell, R. H. Hauge, R. E. Smalley, and R. B. Weisman, Science **298**, 2361 (2002).
[4] A. M. Rao, E. Richter, S. Bandow, B. Chase, P. C. Eklund, K. A. Williams, S. Fang, K. R. Subbaswamy, M. Menon, A. Thess, R. E. Smalley, G. Dresselhaus, and M. S. Dresselhaus, Science **275**, 187 (1997).
[5] A. Jorio, M. A. Pimenta, A. G. Souza Filho, R. Saito, G. Dresselhaus, and M. S. Dresselhaus, New J. Phys. **5**, 139 (2003).
[6] M. S. Strano, J. Am. Chem. Soc. **125**, 16148 (2003).
[7] C. Fantini, A. Jorio, M. Souza, M. S. Strano, M. S. Dresselhaus, and M. A. Pimenta, Phys. Rev. Lett. **93**, 147406 (2004).
[8] H. Telg, J. Maultzsch, S. Reich, F. Hennrich, and C. Thomsen, Phys. Rev. Lett. **93**, 177401 (2004).
[9] A. Jungen, V. N. Popov, C. Stampfer, L. Durrer, S. Stoll, and C. Hierold, Phys. Rev. B **75**, 041405(R) (2007).
[10] R. Pfeiffer, Ch. Kramberger, F. Simon, H. Kuzmany, V. N. Popov, and H. Kataura, Eur. Phys. J. B **42**, 345 (2004).
[11] M. Xia, S. Zhang, X. Zuo, E. Zhang, S. Zhao, J. Li, L. Zhang, Y. Liu, and R. Liang, Phys. Rev. B **70**, 205428 (2004).
[12] A. Rahmani, J.-L. Sauvajol, J. Cambedouzou, and C. Benoit, Phys. Rev. B **71**, 125402 (2005).
[13] R. Pfeiffer, F. Simon, H. Kuzmany, and V. N. Popov, Phys. Rev. B **72**, 161404(R) (2005).
[14] J. Arvanitidis, D. Christofilos, K. Papagelis, T. Takenobu, Y. Iwasa, H. Kataura, S. Ves, and G. A. Kourouklis, Phys. Rev. B **72**, 193411 (2005).
[15] S. Bandow, M. Takizawa, K. Hirahara, M. Yudasaka, and S. Iijima, Chem. Phys. Lett. **337**, 48 (2001).
[16] H. Kataura, Y. Maniwa, T. Kodama, K. Kikuchi, H. Hirahara, K. Suenaga, S. Iijima, S. Suzuki, Y. Achiba, and W. Kraetschmer, Synth. Met. **121**, 1195 (2001).
[17] H. Kataura, Y. Maniwa, M. Abe, A. Fujiwara, T. Kodama, K. Kikuchi, H. Imahori, Y. Misaki, S. Suzuki, and Y. Achiba, Appl. Phys. A: Mater. Sci. Process. **74**, 349 (2002).
[18] M. Abe, H. Kataura, H. Kira, T. Kodama, S. Suzuki, Y. Achiba, K. I. Kato, M. Takata, A. Fujiwara, K. Matsuda, and Y. Maniwa, Phys. Rev. B **68**, 041405(R) (2003).
[19] R. Pfeiffer, H. Kuzmany, Ch. Kramberger, Ch. Schaman, T. Pichler, H. Kataura, Y. Achiba, J. Kurti, and V. Zolyomi, Phys. Rev. Lett. **90**, 225501 (2003).
[20] D. Christofilos, J. Arvanitidis, C. Tzampazis, K. Papagelis, T. Takenobu, Y. Iwasa, H. Kataura, C. Lioutas, S. Ves, and G. A. Kourouklis, Diamond Relat. Mater. **15**, 1075 (2006).
[21] S. Reich and C. Thomsen, Philos. Trans. R. Soc. London, Ser. A **362**, 2271 (2004).
[22] V. N. Popov and L. Henrard, Phys. Rev. B **65**, 235415 (2002).
[23] J. Arvanitidis, D. Christofilos, K. Papagelis, K. S. Andrikopoulos, T. Takenobu, Y. Iwasa, H. Kataura, S. Ves, and G. A. Kourouklis, Phys. Rev. B **71**, 125404 (2005).
[24] U. D. Venkateswaran, Phys. Status Solidi B **241**, 3345 (2004).